

Archiv-Ex.:  
FZR-118  
December 1995  
Preprint

*A. I. Titov, B. Kämpfer,  
B. L. Reznik and V. Shklyar*

The reaction  $NN \rightarrow NN\gamma$  in the  
1 GeV region within an  
effective one-boson exchange model

**Forschungszentrum Rossendorf e.V.**

**Postfach 51 01 19 · D-01314 Dresden**

**Bundesrepublik Deutschland**

**Telefon (0351) 260 3258**

**Telefax (0351) 260 3700**

**E-Mail [kaempfer@fz-rossendorf.de](mailto:kaempfer@fz-rossendorf.de)**

# The reaction $NN \rightarrow NN\gamma$ in the 1 GeV region within an effective one-boson exchange model

A.I. TITOV<sup>1,2,3</sup>, B. KÄMPFER<sup>1,4</sup>, B.L. REZNIK<sup>3</sup>, V. Shklyar<sup>2</sup>

<sup>1</sup>Research Center Rossendorf Inc., Institute for Nuclear and Hadron Physics,  
PF 510119, 01314 Dresden, Germany

<sup>2</sup>Joint Institute for Nuclear Research, Bogoliubov Institute of Theoretical Physics,  
141980 Dubna, Russia

<sup>3</sup>Far Eastern University, 690000 Vladivostok, Russia

<sup>4</sup>Technical University Dresden, Institute of Theoretical Physics,  
Mommstr. 13, 01062 Dresden, Germany

## Abstract

Within an effective one-boson exchange parametrization of the T matrix of  $NN$  interactions we calculate cross sections for the reactions  $pp \rightarrow pp\gamma$  and  $pn \rightarrow pn\gamma$  for proton incidence energies in the order of 1 GeV. Besides bremsstrahlung processes we consider photons from  $\Delta$  decays and contributions from the  $\eta \rightarrow \gamma\gamma$  process, where the  $\eta$  is excited via the  $N_{1535}$  resonance. At beam energies above 700 MeV the  $\Delta$  decay channel dominates for large photon energies, while above the  $\eta$  threshold the  $\eta$  decay photons show up only in a narrow window. The low energy photons stem from pure bremsstrahlung processes.

PACS number(s): 13.75.Cs, 25.20.-x, 25.40.-h

key words: bremsstrahlung, effective one-boson exchange model

The recent first data taking with the time-of-flight (TOF) detector at COSY in Jülich for  $pp$  collisions at kinetic energies  $T_{beam} = 280 - 2500$  MeV stimulates the general interest in  $NN$  reactions in the 1 GeV region. Among the various channels there is the reaction  $NN \rightarrow NN\gamma$ . Previous data on bremsstrahlung photons in  $pp \rightarrow X\gamma$  and  $pn \rightarrow X\gamma$  reactions is restricted to  $T_{beam} \leq 730$  MeV [1], and most studies focus on the data at  $T_{beam} = 280$  MeV [2, 3] and its analysis [4]. At lower energies certainly the potential models for bremsstrahlung (cf. [5]), with appropriate improvements by meson exchange currents and resonance excitations [6, 7], represent suitable tools for understanding the data. At higher energies, however, fully covariant models should be utilized. The envisaged photon production studies with the TOF detector at COSY are particularly interesting, since in an overlapping energy region of  $T_{beam} = 1 - 5$  GeV there exists also data on virtual photon (i.e., di-electron) production [8], which has been quite extensively analyzed (cf. [9, 10, 11]). Therefore, it seems worthwhile to apply the same models to the real photon production to arrive at a coherent picture of electromagnetic processes in the strong interaction of nucleons. Such a task is particularly tempting as there are controversial explanations of peculiarities of the virtual photon production mechanism at  $T_{beam} = 1 - 1.5$  GeV [9, 11]: Either subtle interferences between different channels (including the  $\Delta$ ) or a strong contribution of  $\eta$  Dalitz decays can explain the beam energy dependence of cross sections. Measurements of refined observables [12] might disentangle the various dilepton sources, however, one can also look into the real photon channel to get information on relevant photon production mechanisms.

Here we present first results of our effective one-boson exchange calculations along the lines of Ref. [9] for the reaction  $NN \rightarrow NN\gamma$  which, in contrast to earlier calculations [13, 14], include  $\Delta$  and  $N_{1535}$  excitations too. We are going to present the cross sections  $d\sigma/d\omega$ , and  $d\sigma/d\omega d\Omega$  at fixed  $\omega$ , where the photon energy  $\omega$  and the solid angle  $\Omega$  refer to the  $NN$  center-of-mass system (c.m.s.).

The cross section of the reaction  $N_1 N_2 \rightarrow N_1' N_2' \gamma$  reads

$$\frac{d\sigma}{d\omega d\Omega} = \frac{\omega}{8(2\pi)^5 \sqrt{s(s-4M^2)}} \int |\mathcal{M}_{NN \rightarrow NN\gamma}|^2 D(p') d\Omega_{p'} + \frac{\tilde{B}^{\eta \rightarrow \gamma\gamma} \sigma_\eta}{2\pi} \mathcal{R} \quad (1)$$

where  $D(p') = p'^2 / |Ap' + CE'|$  with  $E' = [AB - C\sqrt{B^2 - M^2(A^2 - C^2)}] / (A^2 - C^2)$ ,  $A = 2(\sqrt{s} - \omega)$ ,  $B = s - 2\omega\sqrt{s}$ ,  $C = 2\omega \cos \Theta_{\vec{p}'\vec{k}}$ . The 3-momentum of the outgoing proton in the c.m.s. is  $\vec{p}'$ , and  $\vec{p}'^2 = E'^2 - M^2$ , where the nucleon mass is denoted by  $M$ .

The matrix elements entering  $\mathcal{M}_{NN \rightarrow NN\gamma}$  contain a subgroup of pure bremsstrahlung

diagrams  $\mathcal{M}_i^b$  with pre-emission and post-emission of a photon with momentum  $k$ , and radiation from internal charged-meson lines; the charge exchange diagrams are included. Our list of the four exchanged mesons  $x$  includes  $\pi^{\pm,0}, \rho^{\pm,0}, \omega, \sigma$ , and the nucleon - meson interaction Lagrangian reads in obvious standard notation  $\mathcal{L}_{int} = ig_\pi \bar{\psi} \gamma_5 \vec{\tau} \psi \vec{\pi} + g_\rho \bar{\psi} \gamma_\mu \vec{\tau} \psi \vec{\rho}^\mu + g_\omega \bar{\psi} \gamma_\mu \psi \omega^\mu + g_\sigma \bar{\psi} \psi \sigma$ . The effective coupling "constants"  $g_x$  change with beam energy according to  $g_x(s) = g_x^0 \exp(-\beta_x \sqrt{s - 4m_x^2})$  [15] with  $\sqrt{s}$  as total c.m.s. energy. The strong  $NNx$  vertices are dressed by formfactors: either for each vertex  $F_{NNx}(q) = (\Lambda_x^2 - m_x^2)/(\Lambda_x^2 - q^2)$  (when the internal meson line  $x$  carries the momentum  $q$ ) or for both vertices  $F_{NNx}(q_1)F_{NNx}(q_2) \left(1 + \frac{m_x^2 - q_1^2}{\Lambda_x^2 - q_1^2} + \frac{m_x^2 - q_2^2}{\Lambda_x^2 - q_2^2}\right)$  (when the internal line radiates a photon with momentum  $k = \pm(q_1 - q_2)$ ); the  $xx\gamma$  vertex is then  $-ie(q_1^\mu + q_2^\mu) \epsilon_\mu^r$  with  $e$  as electromagnetic coupling and  $\epsilon_\mu^r$  as photon polarization 4-vector). If the photon is emitted off a nucleon line the  $NN\gamma$  vertex is as usual  $-ie\gamma^\mu \epsilon_\mu^r$ . The formfactors are constructed in such a way that they preserve gauge invariance [11, 16, 17]. Table 1 lists the meson masses, coupling strengths, and cut-off parameters which are adjusted to the experimental elastic  $NN$  scattering cross section (total and angular dependence) [18].

A second subgroup of contributions  $\mathcal{M}_i^\Delta$  to  $\mathcal{M}_{NN \rightarrow NN\gamma}$  contains the excitation of  $\Delta^{+,0}$  at the strong  $N\Delta\pi$  vertex of the pion exchange and the subsequent decay  $\Delta \rightarrow N\gamma$ . The  $NN \rightarrow N\Delta$  interaction is characterized by the T matrix  $\mathcal{T}^\Delta = g_\Delta (\bar{\psi}_\mu^\Delta \vec{\tau} q^\mu \psi) (\bar{\psi}_\mu^\Delta \vec{\tau} \gamma_5 \gamma^\nu q_\nu \psi) / (m_\pi^2 - q^2) F^2(q^2)$  with the above formfactor with  $\Lambda_\Delta$ . The effective parameter  $g_\Delta^2 = \sigma_\Delta^{WA} / \int \frac{d\sigma_\Delta}{dt} dt$  is normalized with the VerWest - Arndt parametrization of the  $\Delta$  production cross section  $\sigma_\Delta^{WA}$  [19] (the angular differential cross section  $d\sigma_\Delta/dt$  is calculated within our model), and  $\Lambda_\Delta = 0.7$  GeV is fixed by reproducing the cross section  $d\sigma^{pp \rightarrow n\Delta^{++}}/dt$  [20] and the total  $\Delta$  production cross section. Please notice that for these fits no others mesons are needed.

The decay vertex  $\Delta \rightarrow N\gamma$  is parametrized by  $\Gamma_\mu = -ieG_\Delta (\gamma^\nu k_\nu \epsilon_\mu - \gamma^\nu k_\mu \epsilon_\nu) \gamma_5$  with  $G_\Delta = 2.18$ , which results in the decay width  $\Gamma^{\Delta \rightarrow N\gamma} = \tilde{B}^{\Delta \rightarrow N\gamma} \Gamma_\Delta^0$ , where  $\tilde{B}^{\Delta \rightarrow N\gamma} = 6 \cdot 10^{-2}$  is the branching ratio and  $\Gamma_\Delta^0 = 0.12$  GeV denotes the total  $\Delta$  width. The propagator of the  $\Delta$  is used in standard form for Rarita - Schwinger fields, i.e.,  $S_\Delta^{\mu\nu}(p) = -(\gamma^\tau p_\tau + M_\Delta) [g^{\mu\nu} - \frac{1}{3} \gamma^\mu \gamma^\nu - \frac{2}{3} M_\Delta^{-2} p^\mu p^\nu - 3M_\Delta^{-1} (\gamma^\mu p^\nu - p^\mu \gamma^\nu)] / (p^2 - M_\Delta^2 + iM_\Delta \Gamma_\Delta(p^2))$ , with  $M_\Delta = 1.232$  GeV and momentum dependent  $\Delta$  width  $\Gamma_\Delta(p^2)$  as in Ref. [21].

The second term in Eq. (1) refers to processes where at a strong vertex a  $N_{1535}$  is excited (by  $\pi^{\pm,0}, \rho^{\pm,0}, \omega, \sigma$  exchanges) which afterwards decays into a nucleon and an  $\eta$ . We assume that photons from  $\pi^0$  decays need not to be considered, since they can be identified and

subtracted experimentally [1].

We take the branching ratio  $\tilde{B}^{\eta \rightarrow \gamma\gamma'} = 0.39$  of  $\eta \rightarrow \gamma\gamma$  and determine the contribution to the one-photon production cross section by integrating over the second photon momenta  $k'$ . To arrive at a suitable parametrization of such processes we cast the quantity  $\mathcal{R}$  in Eq. (1) into the form

$$\mathcal{R} = \frac{\int d\Omega_{p'} d\varphi_{\eta} \int_{E_{min}(\omega)}^{E_{max}} |\overline{\mathcal{M}_{NN \rightarrow NN\eta}}|^2 D(p') dE_{\eta}}{\int d\Omega_{p'} d\Omega_{\eta} \int_{m_{\eta}}^{E_{max}} |\overline{\mathcal{M}_{NN \rightarrow NN\eta}}|^2 D(p') p_{\eta} dE_{\eta}}, \quad (2)$$

where  $E_{max} = (s + m_{\eta}^2 - 4M^2)/(2\sqrt{s})$ ,  $E_{min}(\omega) = \omega + m_{\eta}^2/(4\omega)$  and  $D(p')$  and  $E'$  are defined as above but now with  $A = 2(\sqrt{s} - E_{\eta})$ ,  $B = s - 2\sqrt{s}E_{\eta} + m_{\eta}^2$ ,  $C = 2p_{\eta} \cos \Theta_{\vec{p}_{\eta}\vec{p}'}$ . The matrix elements are constructed according to the interaction Lagrangian  $\mathcal{L}'_{int} = ig_{\pi}^* \bar{\psi}_* \vec{\tau} \psi \vec{\pi} + g_{\rho}^* \bar{\psi}_* \gamma_5 \gamma_{\mu} \vec{\tau} \psi \vec{\rho}^{\mu} + g_{\omega}^* \bar{\psi}_* \gamma_5 \gamma_{\mu} \psi \omega^{\mu} + g_{\sigma}^* \bar{\psi}_* \gamma_5 \psi \sigma + g_{\eta}^* \bar{\psi}_* \psi \eta$  with the same formfactors as above and  $\psi_*$  as  $N_{1535}$  wave function. Since we normalize our  $\eta$  production cross section (i.e., the denominator in Eq. (2)) to the experimental value  $\sigma_{\eta}$ , we need only the ratios of the couplings, which we take as  $g_{\pi}^* : g_{\rho}^* : g_{\omega}^* : g_{\sigma}^* = 1 : 0.78 : 0.55 : 0.17$  in accordance with Ref. [15]. In our calculations we employ the parametrization  $\sigma_{\eta} = a(1 - \xi^2)/\{(1 + [b(1 - \xi)/\xi]^c)\sqrt{s(s - 4M^2)}\}$  with  $a = 4 \cdot 10^2 \cdot (3 \cdot 10^3)$  mb·GeV<sup>2</sup>,  $b = 17$  (33) and  $c = 1.8$  (2.1) for  $pp$  ( $pn$ ) reactions. The quantity  $\xi$  is defined by  $\xi = \sqrt{s_0/s}$  with  $s_0 = (2M + m_{\eta})^2$ . This parametrization is in agreement with results of [15] and numerically coincides with [22]. Eq. (2) shows that the  $\eta$  decay contributes in the window  $\tilde{\omega}_{min} \leq \omega \leq \tilde{\omega}_{max}$  with  $\tilde{\omega}_{max} = \frac{1}{2}(E_{max} \pm \sqrt{E_{max}^2 - m_{\eta}^2})$ . The virtual  $N_{1535}$  resonance is assumed to be an unstable particle, which is described by replacing  $M \rightarrow M^* - i\frac{1}{2}\Gamma^*$  in the nucleon propagator with  $M^* = 1535$  MeV and  $\Gamma^* = 180$  MeV.

In case of  $pn \rightarrow pn\gamma$  one has  $\mathcal{M}_{NN \rightarrow NN\gamma} = \sum_{i=1}^{14} \mathcal{M}_i^b + \sum_{i=1}^4 \mathcal{M}_i^{\Delta}$  and  $\mathcal{M}_{NN \rightarrow NN\eta} = \sum_{i=1}^{12} \mathcal{M}_i^{N_{1535}}$ , while for  $pp \rightarrow pp\gamma$  the matrix elements read  $\mathcal{M}_{NN \rightarrow NN\gamma} = \sum_{i=1}^{32} \mathcal{M}_i^b + \sum_{i=1}^4 \mathcal{M}_i^{\Delta}$  and  $\mathcal{M}_{NN \rightarrow NN\eta} = \sum_{i=1}^{16} \mathcal{M}_i^{N_{1535}}$ . Spin averaging is performed by utilizing the power of REDUCE in calculating the usual trace expressions in  $|\overline{\mathcal{M}_{NN \rightarrow NN\gamma}}|^2$  and  $|\overline{\mathcal{M}_{NN \rightarrow NN\eta}}|^2$ , where all interference terms are exactly regarded for both  $pn \rightarrow pn\gamma$  and  $pp \rightarrow pp\gamma$ . Multidimensional phase space integrals are performed by Monte Carlo integration. A partial test of our numerical implementation is accomplished by comparing with results of Ref. [14].

Our results are displayed in Figs. 1 ( $pn$ ) and 2 ( $pp$ ) for  $T_{beam} = 700, 1000, 1350$  and 1700

MeV. This energy range covers the expected validity of our model. With increasing beam energy the rôle of  $\Delta$  excitations and  $\eta$  decays becomes more important. Note that  $T_{beam} = 1350$  MeV is just slightly above the  $\eta$  threshold. Let us first consider the reaction  $pn \rightarrow pn\gamma$  (Fig. 1). One can distinguish two regions in the energy-differential cross section in Fig. 1a: At low photon energies the bremsstrahlung dominates, while above  $\omega/\omega_{max} = 0.2 - 0.4$  (with  $\omega_{max} \equiv (s - 4M^2)/(2\sqrt{s})$ ) most photons stem from the  $\Delta$  decays. The magnetic part of the general  $NN\gamma$  vertex contributes preferential at larger photon energies, but here the  $\Delta$  decay anyhow dominates. This justifies our restriction to the pure electric  $NN\gamma$  vertex structure. At  $T_{beam} = 1.7$  GeV there is a narrow window wherein the  $\eta$  decay contribution almost shines out (see Fig. 1a). Interference effects are not important in these spectra, when comparing with the total yield, i.e., one might represent the total cross section in good approximation as incoherent superposition of the pure bremsstrahlung contribution plus the  $\Delta$  decay part plus some  $\eta$  decay yield. The situation changes for the angular distribution at  $T_{beam} = 700$  MeV for  $\omega/\omega_{max} = 0.5$  (Fig. 1b). Here the interference terms become as large as the dominating individual contributions at large angles. (This is in agreement with [11], where the strongest interference effects are found near the kinematical boundary.) Since we keep  $\omega/\omega_{max} \approx 0.5$ , this effect is not seen for higher bombarding energies because the value of  $\omega/\omega_{max}$ , where the bremsstrahlung and  $\Delta$  contributions are equally strong, is changed to smaller numbers.

Similar conclusions hold for  $pp \rightarrow pp\gamma$  (Fig. 2). Here the cross over (Fig. 2a) from the bremsstrahlung to the  $\Delta$  decay-dominated region is sharper. The  $\eta$  contribution is somewhat smaller. Interference terms are smaller than the dominating contributions. The most remarkable fact is the double-humped bremsstrahlung spectrum in the angular distribution (Fig. 2b), which however is hidden under the  $\Delta$  decay contribution. The yield, in comparison to  $pn \rightarrow pn\gamma$ , is suppressed by a factor not larger than four.

The total angular distributions (Figs. 1b and 2b) do not show drastic variations, and it seems difficult to disentangle the different photon sources with these observables.

Our results might be compared with the existing experimental data on  $pp \rightarrow pp\gamma$  [1]. One observes in Fig. 3 a good agreement of our model (without efficiency corrections) with the raw data [1] in the bremsstrahlung region at smaller values of  $\omega$ . (At very small photon energies one recovers the results of the soft photon approximation.) At  $\omega > 100$  MeV the  $\Delta$  contribution becomes dominating which causes an increase of the cross section, in fair agreement with the data. Other elaborate models (e.g., [7]), do not show such a pronounced

cross over to the  $\Delta$  dominated region.

In summary we report a study of photon production within an effective one-boson exchange model which is intended for a prediction of forthcoming data at COSY-TOF. The present results focus on the general theoretical outcome but compare well with existing data. We mention that accurate data on the elastic scattering and the  $\Delta$  contributions are needed to get more confidence in the parameters to be employed. It should be stressed that also the reaction  $pd \rightarrow X\gamma$  is very worth measuring since it complies information on the  $pn$  channel which behaves differently in comparison with the  $pp$  channel, as e.g., seen in the angular distributions.

**Acknowledgments:** Stimulating discussions with E.L. Bratkovskaya, W. Cassing, H. Freiesleben, B. & L. Naumann, P. Michel, K. Möller, and U. Mosel are gratefully acknowledged. The work is supported by BMBF grant 06DR666I, and International Science Foundation grant MP8300.



## References

- [1] B.M.K. Nefkens, O.R. Sander, D.I. Sober, *Phys. Rev.* **38** (1977) 876
- [2] P. Kitching et al., *Phys. Rev. Lett.* **57** (1986) 2363, *Nucl. Phys. A* **463** (1987) 87  
B. v. Przewoski et al., *Phys. Rev. C* **45** (1991) 2001
- [3] K. Michaelian et al., *Phys. Rev. D* **41** (1990) 2689
- [4] F. de Jong, K. Nakayama, T.S.H. Lee, *Phys. Rev. C* **51** (1995) 2334
- [5] V. Herrmann, J. Speth, K. Nakayama, *Phys. Rev. C* **43** (1991) 394  
V. Herrmann, K. Nakayama, *Phys. Rev. C* **45** (1992) 1450
- [6] J.A. Eden, M.F. Gari, *Phys. Lett. B* **347** (1995) 187, preprints RUB-MEP-81/94, 90/95
- [7] M. Jetter, H.W. Fearing, *Phys. Rev. C* **51** (1995) 1666
- [8] W.K. Wilson et al., *Phys. Lett. B* **316** (1994) 245
- [9] B. Kämpfer, A.I. Titov, E.L. Bratkovskaya, *Phys. Lett. B* **301** (1993) 123  
A.I. Titov, B. Kämpfer, E.L. Bratkovskaya, *Phys. Rev. C* **51** (1995) 227
- [10] L.A. Winckelmann, H. Stöcker, W. Greiner, H. Sorge, *Phys. Lett. B* **298** (1993) 22  
K. Haglin, C. Gale, *Phys. Rev. C* **49** (1994) 401
- [11] M. Schäfer, H.C. Dönges, A. Engel, U. Mosel, *Nucl. Phys. A* **575** (1994) 429
- [12] E.L. Bratkovskaya, W. Cassing, U. Mosel, O.V. Ternaev, A.I. Titov, V.D. Toneev, *Phys. Lett. B* **362** (1995) 17
- [13] A. Szyjewicz, A.N. Kamal, *Lecture Notes in Physics* **82** (1978) 88, Springer Verlag, Berlin  
T.S. Biro, K. Niita, A.L. de Paoli, W. Bauer, W. Cassing, U. Mosel, *Nucl. Phys. A* **475** (1987) 579
- [14] M. Schäfer, T.S. Biro, W. Cassing, U. Mosel, H. Niefenecker, J.A. Piston, *Z. Phys. A* **339** (1991) 391  
W. Cassing, V. Metag, U. Mosel, K. Niita, *Phys. Rep.* **188** (1990) 363  
M. Schäfer, Ph. D. thesis, Giessen 1994, unpublished
- [15] T. Vetter, A. Engel, T.S. Biro, U. Mosel, *Phys. Lett. B* **273** (1991) 153
- [16] K.L. Haglin, *Ann. Phys.* **212** (1991) 84
- [17] I.S. Towner, *Phys. Rep.* **155** (1987) 263
- [18] P.J. Carlson et al., in vol. 7, *Landolt-Börnstein*, Berlin 1973
- [19] B.J. VerWest, R.A. Arndt, *Phys. Rev. C* **25** (1982) 1979
- [20] A.M. Eisner, E.L. Hart, R.I. Louttit, T.W. Morris, *Phys. Rev.* **138** (1965) B670
- [21] W. Weise, *Nucl. Phys. A* **278** (1977) 402  
V. Dimitriev, O. Shushkov, C. Gaarde, *Nucl. Phys. A* **459** (1989) 503
- [22] A.L. de Paoli et al., *Phys. Lett. B* **219** (1989) 194  
E. Chiavassa et al., *Phys. Lett. B* **322** (1994) 270

Fig. 1: The differential cross sections  $\omega d\sigma/d\omega$  vs.  $\omega/\omega_{max}$  (a), and  $\omega d\sigma/d\omega d\Omega$  vs.  $\vartheta$  at  $\omega/\omega_{max} = 0.5$  (b) for the reaction  $pn \rightarrow pn\gamma$  at  $T_{beam} = 700, 1000, 1350,$  and  $1700$  MeV (triangles: bremsstrahlung, squares:  $\Delta$  decay, circles:  $\eta$  decays, crosses: interference of bremsstrahlung and  $\Delta$  decay, heavy full lines: total cross section).

$pn$

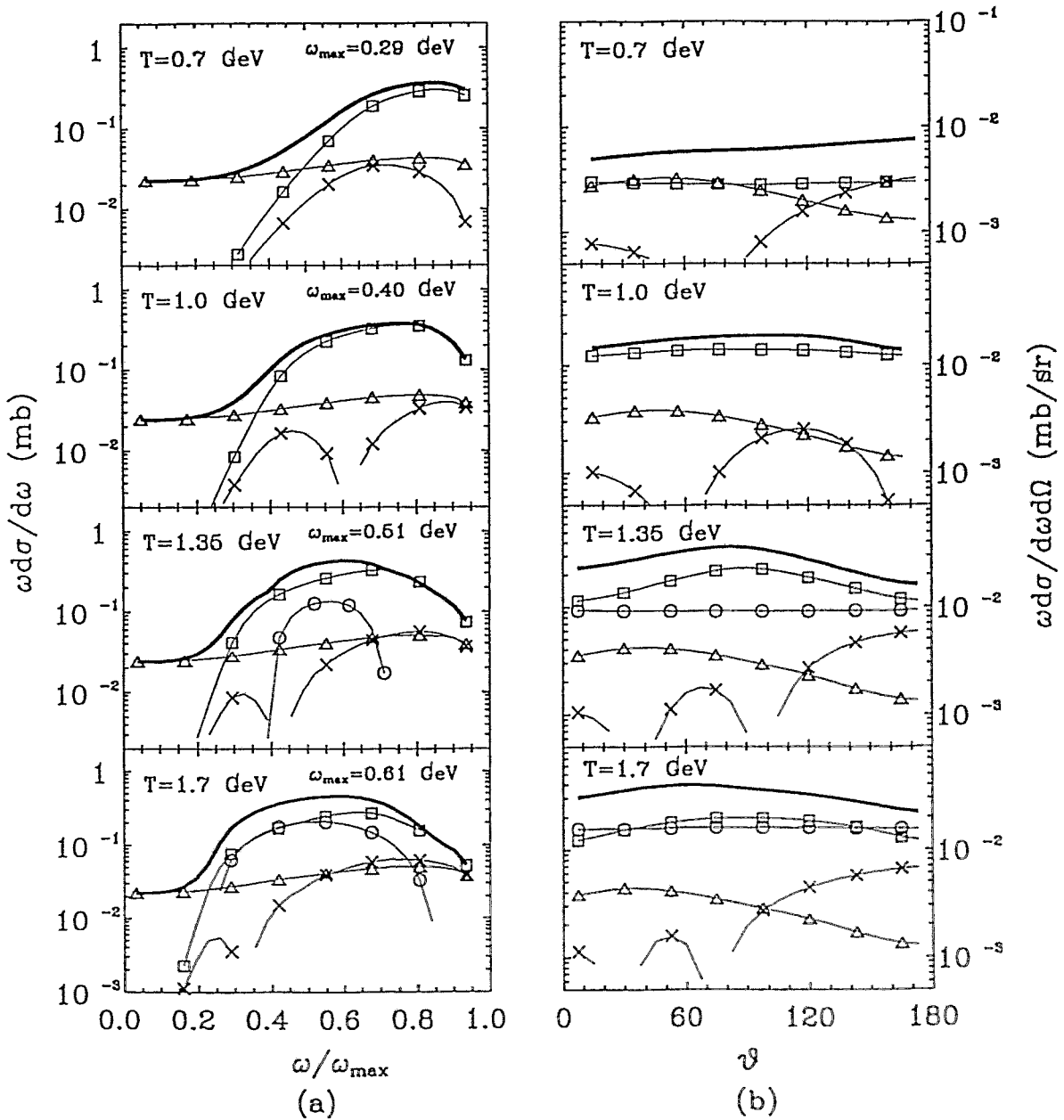


Fig.1

Fig. 2: The same as Fig. 1 but for  $pp \rightarrow pp\gamma$ .

$pp$

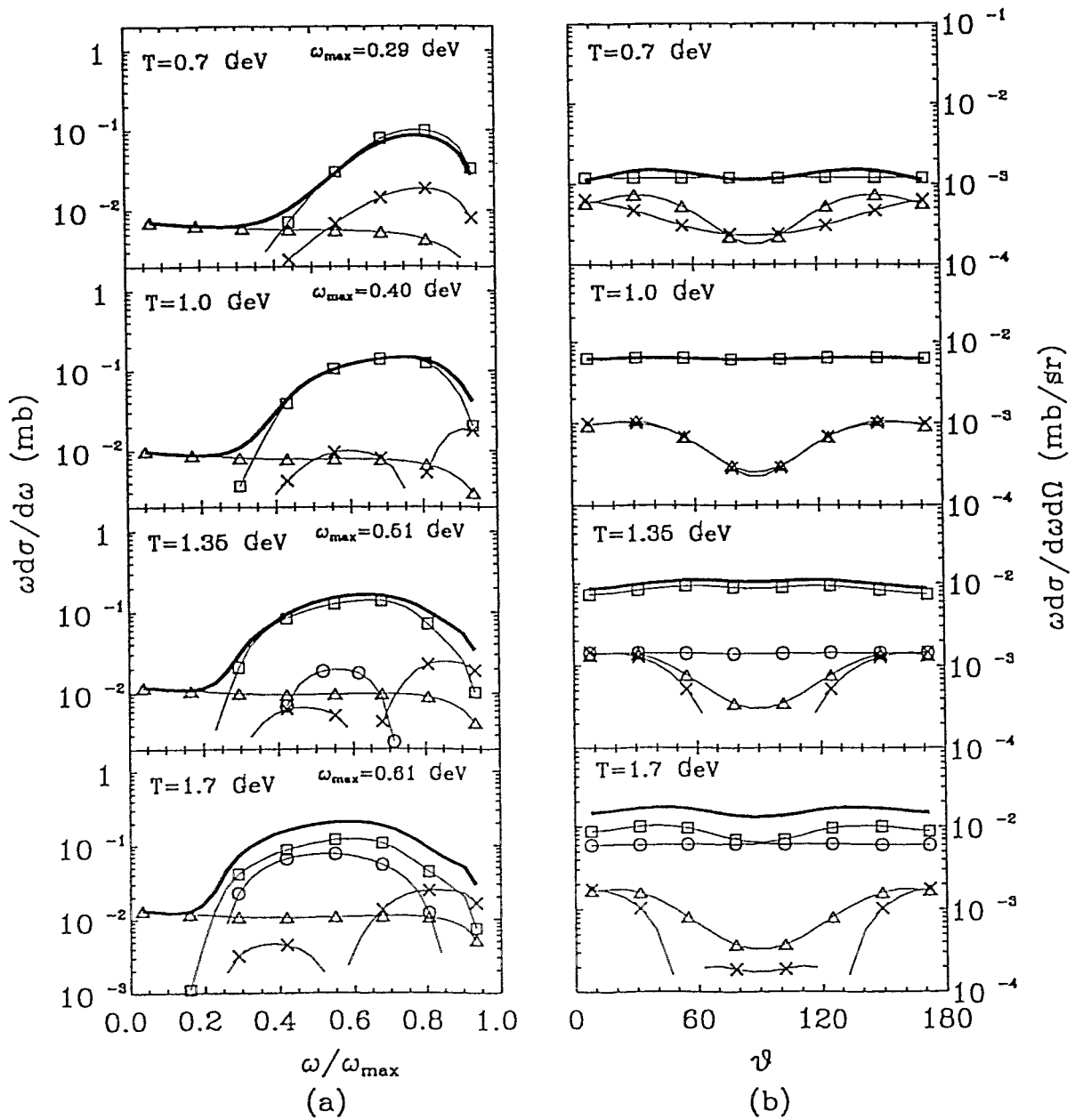


Fig.2

Fig. 3: Comparison of our calculations with experimental data of the reaction  $p(730 \text{ MeV})p \rightarrow pp\gamma$  measured with the counter  $G_{10}$  [1] (dot-dashed curve: soft photon approximation, long-dashed curve: bremsstrahlung, short-dashed curve:  $\Delta$  contribution, heavy full curve: the total cross section).

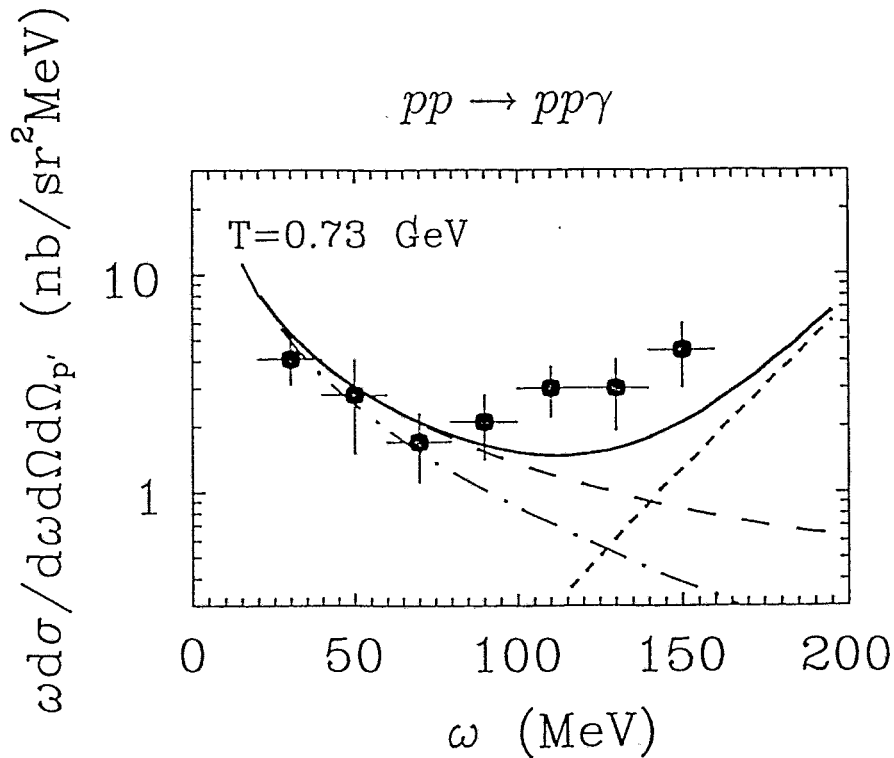


Fig.3

Table 1: The parameter set used in the present work.

meson	mass	coupling	cut-off	energy parameter
$x$	$m_x$ [MeV]	$g_x^0$	$\Lambda_x$ [GeV]	$\beta_x$
$\pi$	138	12.23	1.0	0.046
$\rho$	630	1.78	1.6	0.047
$\omega$	782	10.08	1.2	0.046
$\sigma$	550	2.58	1.6	0.041